Thermodynamic Control of Intramolecular Singlet Fission and Exciton Transport in Linear Tetracene Oligomers

Nakamura, Shunta ; Sakai, Hayato ; Fuki, Masaaki ; Ooie, Rikuto ; Ishiwari, Fumitaka ; Saeki, Akinori ; Tkachenko, V. Nikolai ; Kobori,…

(Citation)
Angewandte Chemie International Edition,62(8):e202217704

(Issue Date)
2022-12-28

(Resource Type)
journal article

(Version)
Accepted Manuscript

RESEARCH ARTICLE

Thermodynamic Control of Intramolecular Singlet Fission and Exciton-Transport in Linear Oligomeric Forms

Shunta Nakamura,[a] Hayato Sakai,[a] Masaaki Fuki,[b,c] Rikuto Ooie,[d] Fumitaka Ishiwari,[d,e] Akinori Saeki,[d,e] Nikolai V. Tkachenko,*[f] Yasuhiro Kobori*[b,c] and Taku Hasobe*[a]

[a] Dr. S. Nakamura, Dr. H. Sakai, Prof. Dr. T. Hasobe
Department of Chemistry, Faculty of Science and Technology, Keio University, Yokohama, Kanagawa223-8522 (Japan)
E-mail: hasobe@chem.keio.ac.jp
[b] Dr. M. Fuki, Prof. Dr. Y. Kobori
Molecular Photoscience Research Center, Kobe University, 1-1 Rokkodai-cho, Nada-ku, Kobe 657-8501 (Japan)
E-mail: ykobori@kitty.kobe-u.ac.jp
[c] Dr. M. Fuki, Prof. Dr. Y. Kobori
Department of Chemistry, Graduate School of Science, Kobe University, 1-1, Rokkodai-cho, Nada-ku, Kobe 657-8501 (Japan)
E-mail: ykobori@kitty.kobe-u.ac.jp
[d] R. Ooie, Dr. F. Ishiwari, Prof. Dr. A. Saeki
Department of Applied Chemistry, Graduate School of Engineering, Osaka University, Suita, Osaka 565-0871 (Japan)
[e] Dr. F. Ishiwari, Prof. Dr. A. Saeki
Innovative Catalysis Science Division, Institute for Open and Transdisciplinary Research Initiatives (ICS-OTRI), Osaka University, Suita, Osaka 565-0871 (Japan)
[f] Prof. Dr. N. V. Tkachenko
Chemistry and Advanced Materials Group, Faculty of Engineering and Natural Sciences, Tampere University, Korkeakoulunkatu 8, FI33720 Tampere (Finland)
E-mail: nikolai.tkachenko@tuni.fi

Abstract: We newly synthesized a series of homo- and hetero-tetracene (Tc) oligomers to propose a molecular design strategy for the efficient exciton-transport in linear oligomers by promoting correlated triplet pair (TT) dissociation and controlling sequential exciton-trapping process of individual doubled triplet excitons (T+T) at terminal positions by intramolecular singlet fission. First, entropic gain effects on the number of Tc units are examined by comparing Tc-homo-oligomers [$(Tc)_n$: n = 2, 4, 6]. Then, a comparison of $(Tc)_n$ and Tc-hetero-oligomer [TcF_3-$(Tc)_4$-TcF_3] reveals the vibronic coupling effect for entropic gain. Observed entropic effects on the T+T formation indicated that the exciton-migration is rationalized by number of possible TT states increased both by increasing the number of Tc units and by the vibronic levels at the terminal TcF_3. Finally, we successfully observed high-yield exciton-trapping process at terminal units [i.e., $^3TcF_3^*$-$(Tc)_4$-$^3TcF_3^*$] (trapped triplet yield: Φ_{TrT} = 176 ± 8%).

Introduction

Exciton generation and subsequent transport processes in molecular assemblies are associated with various photoenergy utilization processes such as photosynthetic light-harvesting complexes,[1] photovoltaics and photocatalysis,[2] light-emitting diodes[3] and quantum information science.[4] One of the ways for improving exciton-transport process is to design and synthesize the one-dimensional linear oligomers or polymers. Among them, many singlet exciton-transport processes have been widely reported.[5] In contrast, the utilization of long-lived excited triplet states is required for long-range exciton-transport process because the exciton-diffusion length is associated with the lifetimes of the excited states.[6] However, the formation of efficient triplet excitons is extremely difficult because intersystem crossing (ISC) is generally a spin-forbidden reaction.

A solution to the above problem is the utilization of singlet fission (SF).[7] SF is a spin-allowed photophysical process which is able to generate two individual triplet states (T+T) from one-photon absorption through a correlated triplet pair (TT) in two nearby chromophores.[8] For example, 5,12-bis((triisopropylsilyl)ethynyl)tetracene (TIPS-tetracene) meets the energy level matching condition between the lowest-lying singlet excited state ($E(S_1)$ = 2.3 eV) and two triplet excited states ($E(T_1)$ = 1.25 eV) [i.e., $E(S_1) \geq 2E(T_1)$], and our group reported the quantitative individual triplet generation by intramolecular SF (ISF) utilizing biphenyl linker-bridged Tc dimers.[9]

A few recent ISF systems demonstrated the effects of the spatially separated and conformationally disordered T+T geometries on the enhancements of ISF utilizing linear oligomers (i.e., "energy cleft" model).[10] It is spatially dependent, but also electronically biased energy diffusion towards the terminal acceptor units. Note that these simply demonstrated the improvement of TT dissociation process from the strongly coupled exciton pair in either homo-oligomers or hetero-oligomers. It is desired to molecularly understand the exciton-transport mechanism in connection to vibration-induced process by ISF, but no such case has been reported.

It should be further emphasized that we already succeeded in the generation of weakly correlated TT and observation of the efficient TT dissociation process by utilizing 2,2'-biphenyl linker-bridged tetracene dimer in which specific vibration motions play a role.[11] This is distinguished from the above energy cleft model by simple exciton hopping in oligomers during the dissociation. In addition to the entropic effect for the hole-dissociation after primary photoinduced charge-separation in a series of poly(3-hexylthiophene)–fullerene linked dyads,[12] we reported the enthalpy-entropy compensation effect on the TT dissociation process in a series of pentacene and hexacene dimers, suggesting importance of the specific vibrations for dissociations.[13] Therefore, it is expected that the mechanisms of the TT dissociation and exciton-transport processes can be clarified by determining the thermodynamic parameters utilizing a series of homo-and hetero-oligomers with a variety of number of the linking chromophores (Figure 1).

Based on the above concepts, we propose a molecular design strategy for the efficient exciton-transport process in molecular assemblies by promoting TT dissociation in linear oligomers and controlling subsequent exciton-trapping processes at terminal position of oligomers.

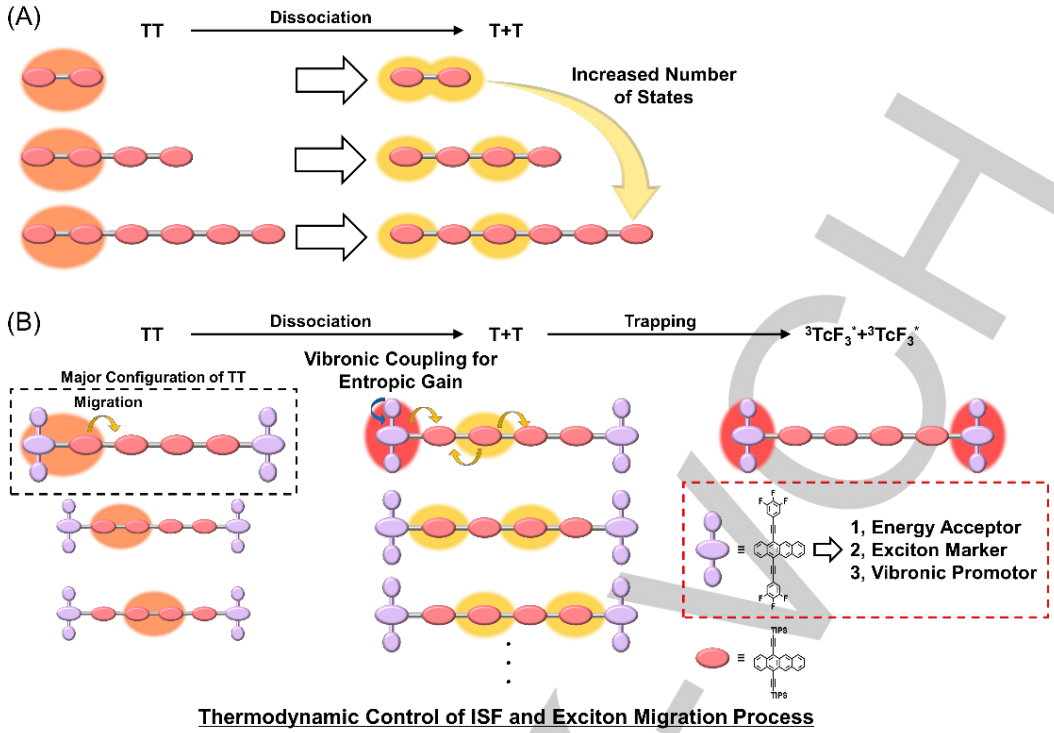

Scheme 1. Conceptual schemes (A) for the TT dissociation in a Tc-homo-oligomers and (B) for the exciton-migration including TT dissociation and exciton-trapping in a Tc-hetero-oligomer.

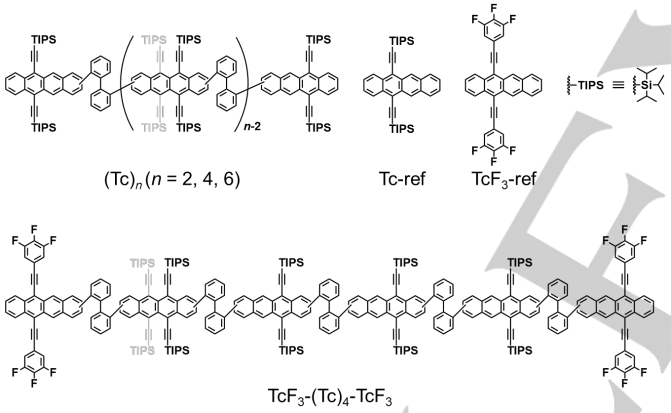

Figure 1. Chemical structures of Tc-oligomers and reference compounds in this study.

We newly synthesized a series of Tc-oligomers bridged by 2,2'-biphenylene spacers (Figure 1). First, entropic gain effects on the number of Tc units are examined by comparing Tc-homo-oligomers [(Tc)$_n$: n = 2, 4, 6]. Then, a comparison of Tc-homo-oligomers [(Tc)$_n$] and Tc-hetero-oligomer [TcF$_3$-(Tc)$_4$-TcF$_3$] reveals the vibronic coupling effect for entropic gain (Figure 1). As described above, a systematic comparison of homo-oligomers and hetero-oligomer enables to clarify the effect of oligomerization on the TT dissociation. Finally, we discuss the exciton-trapping process at terminal units in Tc-hetero-oligomer. In our present system, unlike the above reported systems,[10] T+T is efficiently generated from the weakly correlated TT, and the TT dissociation and subsequent exciton-transport of T+T can be discussed independently. Regarding the design of TcF$_3$-(Tc)$_4$-TcF$_3$, 3,4,5-trifluorophenyl group modified-Tc (TcF$_3$) units were linked at the terminal positions instead of the bis-triisopropylsilylethynyl (TIPS) groups in Tc. The three specific roles for TcF$_3$ are as follows: energy acceptor, exciton marker and vibronic promotor (i.e., torsional motion of trifluorophenyl) (Scheme 1).

Results and Discussion

Synthesis of Tc-oligomers.

Scheme 2 summarized the synthetic procedures of TcF$_3$-(Tc)$_4$-TcF$_3$. It was successfully obtained by repeating Suzuki-Miyaura cross-coupling as a key reaction. The synthetic details of related compounds including Tc-oligomers are described together with their characterizations in experimental section (Schemes S1-S4, Figures S1-S50) in Supporting Information (SI). Considering the linkage form between the Tc and biphenyl spacer units, several structural isomers are possible. However, since the exact isolation was impossible, they were used as is. According to the recent results of tetracene-based oligomers and polymers,[14] no differences of the photophysical processes were observed in different isomers. The temperature-dependent ^{1}H NMR spectra of TcF$_3$-(Tc)$_4$-TcF$_3$ and (Tc)$_6$ also demonstrated no spectral change (Figures S51-S52). This suggested the linear conformation of TcF$_3$-(Tc)$_4$-TcF$_3$ and (Tc)$_6$ in solution together with the optimized structure by DFT calculation (Figure S53).

Steady-state Spectroscopies of Tc-oligomers.

Absorption spectra of Tc-homo-oligomers [(Tc)$_6$, (Tc)$_4$ and (Tc)$_2$] became broadened and red-shifted together with the increased molar absorption coefficients as compared to Tc-ref because of the oligomeric forms (Figure 2A). The spectra of TcF$_3$-ref and TcF$_3$-(Tc)$_4$-TcF$_3$ were similarly broadened and red-shifted as compared to Tc-ref and (Tc)$_6$ because of the introduction of the electron-withdrawing 3,4,5-trifluorophenyl units (Figure 2A and Figure S54). The fluorescence spectral trends are similar to the corresponding absorption spectra (Figure 2B and Figure S55).

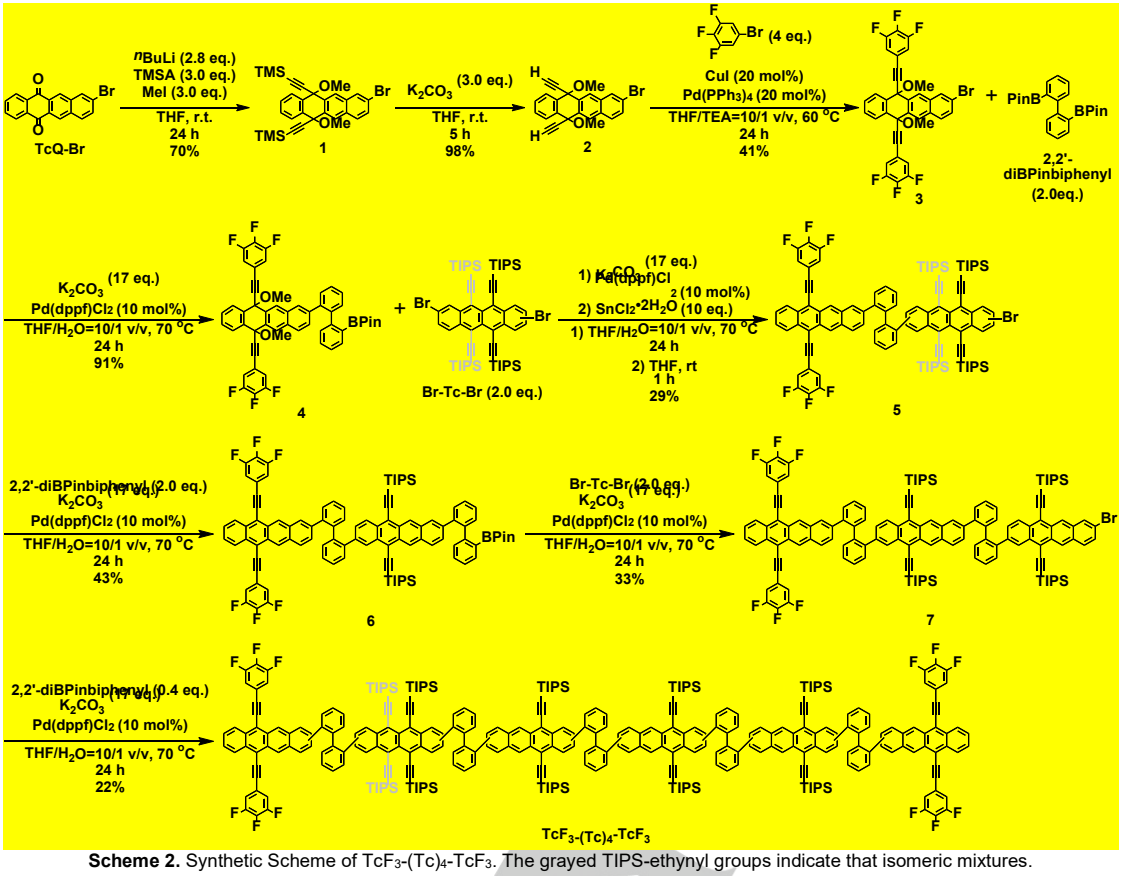

Scheme 2. Synthetic Scheme of TcF_3-$(Tc)_4$-TcF_3. The grayed TIPS-ethynyl groups indicate that isomeric mixtures.

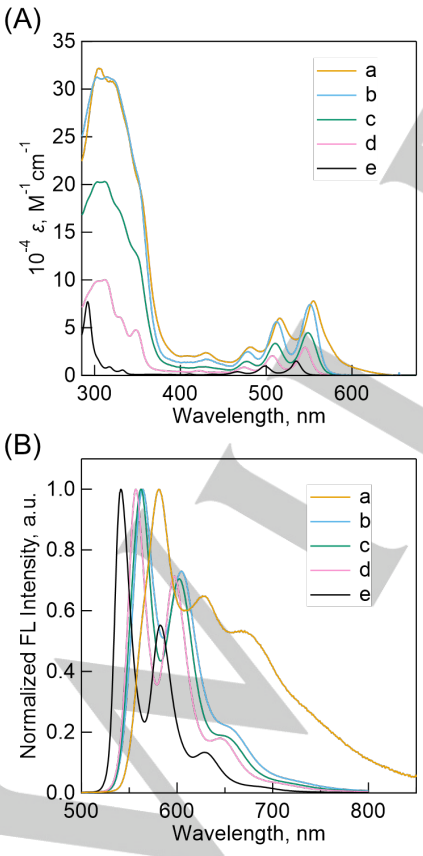

Figure 2. (A) Steady-state absorption spectra of (a) TcF_3-$(Tc)_4$-TcF_3, (b) $(Tc)_6$, (c) $(Tc)_4$, (d) $(Tc)_2$ and (e) Tc-ref in toluene. (A) Steady-state fluorescence spectra of (a) TcF_3-$(Tc)_4$-TcF_3, (b) $(Tc)_6$, (c) $(Tc)_4$, (d) $(Tc)_2$ and (e) Tc-ref in toluene (λ_{ex} = 470 nm).

Theoretical calculations support that TcF_3 acts as the energy acceptor relative to Tc (Figure S56, Table S1). Furthermore, the HOMO and LUMO of TcF_3-ref are both delocalized at the trifluorophenyl substituents as compared to Tc-ref (Figure S56). Therefore, vibronic coupling of trifluorophenyl unit can be considered. This is because the torsional motions in the trifluorophenyl units can cause the increased number of the T+T dissociated state, as a result of the coupling between the vibration levels and the electronic orbital distributions, i.e., the vibronic coupling. In addition, the number of TT activation states can also be increased by this torsional disorder to weaken the electronic couplings in the TT state, contributing to the activation entropy. Moreover, we calculated the difference of the potential energy with rotating 3,4,5-trifluorophenyl units (Figure S57). The calculated rotational barrier was small enough for the vibronic motion. This suggests TcF_3-ref is a useful unit promoting the vibronic motion in the exciton-transport process.

Transient Absorption Spectroscopies of Tc-oligomers.

To investigate ISF, first, femtosecond transient absorption (fsTA) measurements were performed in toluene. The excitation wavelength was 470 nm to populate the higher vibrational level of the lowest excited singlet state of Tc. Separately, triplet-triplet (T-T) and singlet-singlet (S-S) absorption spectra of Tc were measured (Figures S58-S63). The S-S absorption of Tc were confirmed by fsTA of Tc-ref (Figure S63). The corresponding molar absorption coefficients of T-T absorption (ε_T) were determined for the calculation of individual triplet quantum yields (Φ_T) (Figures S58-S62, Tables S2-S5). Note that T-T absorption spectrum of TcF_3-ref is rather different form that of Tc-ref (Figure 3, Figures S58 and S63). This indicates that TcF_3 is a good exciton marker for directly evaluating the exciton-trapping at terminal positions in TcF_3-$(Tc)_4$-TcF_3 (*vide infra*).

Table 1. Summarized Kinetic Parameters at 293 K.

Compound	k_{ISF0} [a] (10^{11} s^{-1})	k_{ISF} [a] (10^{9} s^{-1})	k_{TTA} [a] (10^{8} s^{-1})	k_{Diss} [b] (10^{7} s^{-1})	k_{Rec} [b] (10^{6} s^{-1})	k_{Back} [b] (10^{6} s^{-1})	k_T [c] (10^3 s^{-1}) [τ_T [c] (ms)]	k_{Trap} [b] (10^{6} s^{-1})	k_{TrT} [d] (10^3 s^{-1}) [τ_{TrT} [d] (ms)]	Φ_T (%)	Φ_{TrT} (%)
$(Tc)_2$	1.5	6.2	3.0	5.5	16	4.7	3.7 (0.27)	–	–	165 ± 6 [e]	–
$(Tc)_4$	1.5	6.3	3.0	6.5	13	3.7	3.0 (0.33)	–	–	173 ± 9 [e]	–
$(Tc)_6$	1.4	6.9	2.9	7.2	10	2.6	2.7 (0.37)	–	–	182 ± 10 [e]	–
TcF_3-$(Tc)_4$-TcF_3	1.9	5.4	3.0	9.2	9.0	1.6	2.9 [b]	9.8	3.3 (0.30)	–	176 ± 8 [e]
Tc-ref	–	–	–	–	–	–	3.4 (0.29)	–	–	5 ± 3 [f]	–
TcF_3-ref	–	–	–	–	–	–	3.2 (0.31)	–	–	5 ± 5 [f]	–

[a] Estimated by target analysis of fsTA. [b] Estimated by target analysis of psTA. [c] Calculated by $k_T = (\tau_T)^{-1}$. τ_T was estimated by nsTA. [d] Calculated by $k_{TrT} = (\tau_{TrT})^{-1}$. τ_{TrT} was estimated by nsTA in TcF_3-$(Tc)_4$-TcF_3. [e] Estimated by psTA. [f] Estimated by nsTA.

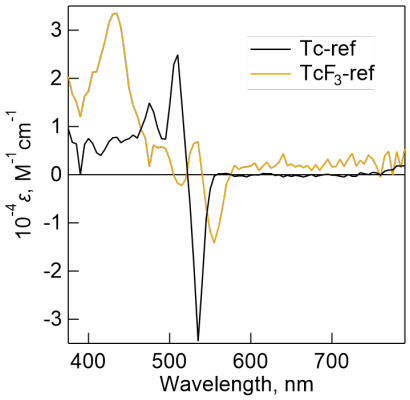

Figure 3. Sensitized T-T absorption spectra of Tc-ref (λ_{ex}: 355 nm, sensitizer: anthracene) and TcF_3-ref (λ_{ex}: 355 nm, sensitizer: C_{60}) in toluene.

fsTA of Tc-homo-oligomers in toluene are shown in Figures S64-S66. Here we discuss $(Tc)_6$ as a typical example. S-S absorption bands initially appeared in the range of ca. 400-450 and 600-750 nm (Figure S64B) through the higher singlet excited states, namely, '*hot S* state*' after photo-excitation. Then, the T-T bands appeared at 500-530 nm together with the decreased S-S bands (Figure S64B). Such a fast singlet-triplet conversion should be attributable to ISF. Note that a competitive reaction between SF and triplet-triplet annihilation (TTA) occurred in the present systems.[11, 15] fsTA of $(Tc)_2$ and $(Tc)_4$ also suggest ISF (Figures S65-S66).

To confirm the direct evidence of TT generation and dissociation, time-resolved paramagnetic resonance (TREPR) study was performed (Figure 4, Figure S67, Table S6). Consequently, the electron spin polarization (ESP) of the microwave absorption (A) and emission (E) in the quintet state ^{5}(TT) and the dissociated states were observed in $(Tc)_6$ and TcF_3-$(Tc)_4$-TcF_3. The E/A/E/A pattern polarization in the quintet was explained by vibronic effects considering the varying exchange interaction (J) in TT coupled to the TT conformation after ISF, as shown by the red line in Figure 4,[15b, 16] indicating that vibration motions play a role for the quintet ^{5}(TT) generations caused by modulation of the J rather than by the exciton-hopping from the $^5(T+T)_0$ back to $^5(TT)_0$ with the assist of the SQ_0 mixing (Figure 4B).[17] Nevertheless, structural difference between the orthogonal ^{5}(TT) configuration and the distorted T+T was explained by the hopping dissociation leading to the ~10^4 fold decrease in the magnitude of J in Table S6.

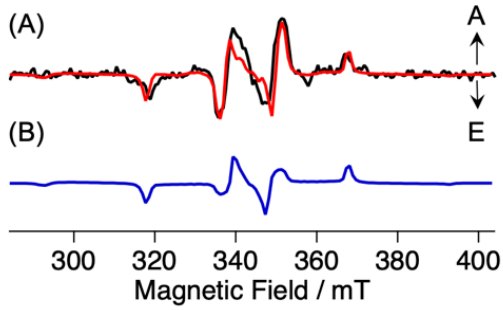

Figure 4. (A) TREPR spectrum of $(Tc)_6$ (λ_{ex}: 532 nm) at 0.3 μs showing the quintet TT state at the center field and dissociated T+T as the spin correlated triplet pair at the outer fields at T = 80 K in 2-methyltetrahydrofuran. Simulated electron spin polarization with the varying exchange coupling model is shown by the red line. (B) Calculated electron spin polarization by the model of the singlet-quintet conversion during the triplet diffusion and subsequent reencounter processes in the multiexciton without considering the vibration motions coupling to the exchange interactions.

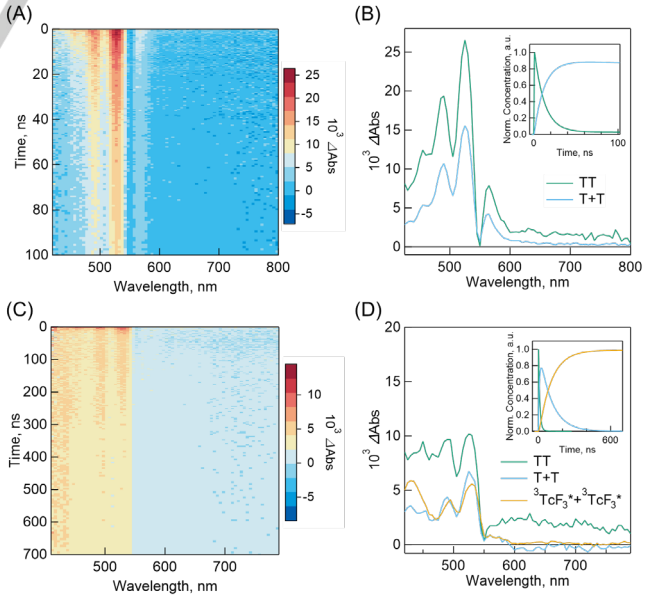

Figure 5. (A) psTA spectra of $(Tc)_6$ in toluene (λ_{ex}: 355 nm). (B) Species-associated spectra (SAS) of $(Tc)_6$. The inset shows decay profiles of TT (green) and T+T (blue). (C) psTA spectra of TcF_3-$(Tc)_4$-TcF_3 in toluene (λ_{ex}: 355 nm). (D) SAS of TcF_3-$(Tc)_4$-TcF_3. The inset shows decay profiles of TT (green), T+T (blue) and $^3TcF_3^*$+$^3TcF_3^*$ (orange).

Table 2. Summarized Thermodynamic Parameters regarding TT Dissociation.

Compound	$\Delta H^{\ddagger}$ [a] (kJ·mol^{-1})	$\Delta S^{\ddagger}$ [a] (J·mol^{-1}·K^{-1})	$\Delta G^{\ddagger}$ at 293 K [b] (kJ·mol^{-1})	$\Delta\Delta W^{\ddagger}$ [c]	ΔH [d] (kJ·mol^{-1})	ΔS [d] (J·mol^{-1}·K^{-1})	ΔG at 293 K [e] (kJ·mol^{-1})	$\Delta\Delta W$ [f]
$(Tc)_2$	3.09 ± 0.09	−86.2 ± 0.3	25.7 ± 0.1	1.00 ± 0.03	1.00 ± 0.10	23.7 ± 0.3	−6.00 ± 0.14	1.00 ± 0.02
$(Tc)_4$	3.12 ± 0.07	−84.2 ± 0.2	25.1 ± 0.1	1.28 ± 0.03	1.00 ± 0.08	27.7 ± 0.3	−6.98 ± 0.12	1.62 ± 0.04
$(Tc)_6$	3.16 ± 0.07	−83.0 ± 0.3	24.7 ± 0.1	1.46 ± 0.03	1.00 ± 0.10	31.9 ± 0.4	−8.21 ± 0.15	2.70 ± 0.07
TcF_3-$(Tc)_4$-TcF_3	3.33 ± 0.03	−80.8 ± 0.1	24.1 ± 0.1	1.90 ± 0.04	0.78 ± 0.07	36.2 ± 0.2	−9.85 ± 0.10	4.52 ± 0.10

[a] Estimated by the Eyring plots (Figure S92A). [b] Calculated by $\Delta G^{\ddagger} = \Delta H^{\ddagger} - T\times\Delta S^{\ddagger}$. [c] Calculated by $\Delta S^{\ddagger} - \Delta S^{\ddagger}_{(Tc)2} = k_B\cdot\ln\Delta W^{\ddagger} - k_B\cdot\ln\Delta W^{\ddagger}_{(Tc)2} = k_B\cdot\ln\Delta\Delta W^{\ddagger}$. ($W$ is number of states. $\Delta W^{\ddagger} = W^{\ddagger}/W_{TT}$, $\Delta\Delta W^{\ddagger} = \Delta W^{\ddagger}/\Delta W^{\ddagger}_{(Tc)2}$). [d] Estimated by the plots of ΔG vs. Temperature (Figure 6B). [e] Calculated by $\Delta G = -RT\ln(k_{Diss}/k_{Back})$. [f] Calculated by $\Delta S - \Delta S_{(Tc)2} = k_B\cdot\ln\Delta W - k_B\cdot\ln\Delta W_{(Tc)2} = k_B\cdot\ln\Delta\Delta W$. ($W$ is number of states. $\Delta W = W_{T+T}/W_{TT}$, $\Delta\Delta W = \Delta W/\Delta W_{(Tc)2}$).

We can propose the kinetic model in Tc-homo-oligomers (Scheme 3A). The rate constant of initial transition process from hot S* to S_1 is denoted as k_{nr}. Then, the direct ISF from hot S* to TT (k_{ISF0}), deactivation process from S_1 (k_0), endergonic ISF (k_{ISF}) from S_1 to TT, and TTA (k_{TTA}) from TT to S_1 are included. In addition to the recombination process (k_{Rec}) from TT to the ground state and deactivation process (k_T) from T+T to the ground state, the TT can generate the T+T by dissociation process (k_{Diss}) together with the reverse process of TT dissociation (k_{Back}). To carefully discuss these kinetic processes, we analyzed the species-associated spectra (SAS) of fsTA (Figures S64C-S66C). SAS and corresponding rate constants were obtained as a result of target analysis (Table 1, Table S7, Figures S68-S69).[18] The k_{TTA} of all systems were an order of magnitude smaller than k_{ISF}. These results indicate that the oligomeric forms maintain the larger rate constants of TT generation relative to the reverse TTA.

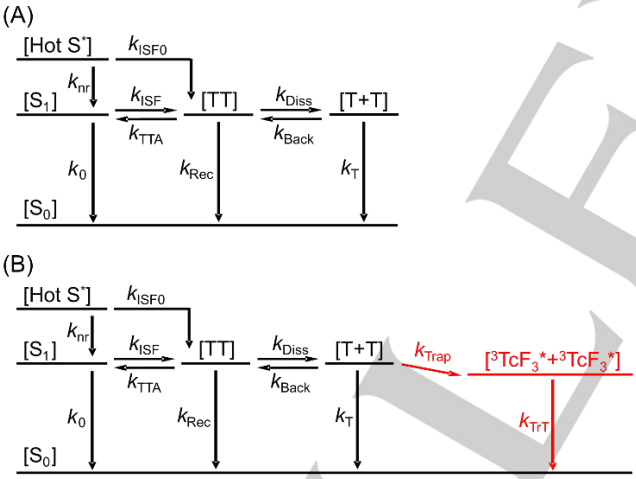

Scheme 3. Proposed Kinetic Schemes for (A) Tc-Homo-Oligomers and (B) TcF_3-$(Tc)_4$-TcF_3.[19]

To evaluate the dissociation of TT in Tc-homo-oligomers, picosecond transient absorption (psTA) of $(Tc)_6$ were measured in toluene with 355 nm excitation (Figures 5A-B, Figure S70). We observed the appearance and prompt decay of TT in the range from 400-450 nm (ca. 1-8 ns) together with $(Tc)_4$ and $(Tc)_2$ (Figures S71-S72). The k_{Diss} was 7.2×10^7 s^{-1} for $(Tc)_6$ and these values increases with increasing the number of Tc (Table 1). Similarly, the individual triplet yields (Φ_T) were 182% for $(Tc)_6$, 173% for $(Tc)_4$ and 165% for $(Tc)_2$, respectively (Table 1, Table S3), which indicates that the Φ_T increases with increasing the number of Tc. Although the direct observation of exciton-migration was unclear, we successfully observed the high-yield Φ_T in $(Tc)_6$ and oligomeric effect in Tc-homo-oligomers.

Next, fsTA of TcF_3-$(Tc)_4$-TcF_3 was measured (Figures S73-S75) together with the kinetic model (Scheme 3B). The differences from the above Tc-homo-oligomers are the exciton-trapping process (k_{Trap}) from T+T to $^3TcF_3^*+^3TcF_3^*$ and the deactivation process from $^3TcF_3^*+^3TcF_3^*$ to the ground state (k_{TrT}). Similarly, we analyzed the SAS of fsTA (Figure S73C). The k_{ISF0} (1.9×10^{11} s^{-1}) and k_{ISF} (5.4×10^9 s^{-1}) are approximately similar to those of Tc-homo-oligomers, indicating that fast ISF occurs even though the energy acceptors are attached at the terminal positions. Then, to evaluate the exciton-migration including TT dissociation and exciton-trapping, psTA of TcF_3-$(Tc)_4$-TcF_3 were examined (Figure 5C-D, Figure S76-S77). In contrast to Tc-homo-oligomers, the following three SAS corresponding to TT, T+T and $^3TcF_3^*+^3TcF_3^*$ were required in TcF_3-$(Tc)_4$-TcF_3 (Figure 5D). This TT should include the $^3TcF_3^*$ species because of the difference in the green-lines between Figure 5D and 5B indicating that the major configuration of TT is populated at the terminus position [$^3Tc^*$-$^3TcF_3^*$] in the time range of a few to 200 nanoseconds. In contrast, the spectral shape of T+T is rather similar to the spectra of ^{3}Tc-ref* and T+T in $(Tc)_6$ (blue-line in Figure 5D). Thus, T+T is mostly composed of the separated $^3Tc^*+^3Tc^*$ at the core $(Tc)_4$ unit in TcF_3-$(Tc)_4$-TcF_3, indicating that the major pathway of intramolecular dissociation occurs from the strongly coupled TcF_3-$(Tc)_3$-$^3Tc^*$-$^3TcF_3^*$ at the terminus positions. More importantly, comparing the orange and blue SASs in Figure 5D, the peak at ca. 420 nm increased with time compared to that at ca. 540 nm, indicating that the two triplet excitons are likely to eventually reach the terminal TcF_3 units (Figure S76). Thus, the localized triplet excitons at the terminal positions of TcF_3-$(Tc)_4$-TcF_3 ($^3TcF_3^*+^3TcF_3^*$), i.e., the exciton-trapping process, was finally confirmed. The k_{Trap} (9.8×10^6 s^{-1}) is 10^3 times greater than that of k_T together with efficient trapped triplet yield (Φ_{TrT} = 176 ± 8%) (Table 1). These results should provide strong evidence for the exciton-migration of TT dissociation (Scheme 1). Additionally, the k_{Diss} (9.2×10^7 s^{-1}) for TcF_3-$(Tc)_4$-TcF_3 is larger than those in Tc-homo-oligomers. This may suggest that a vibronic effect by TcF_3 promotes the TT dissociation, as detailed below. Additionally, we also measured and analyzed fsTA and psTA spectra of TcF_3-$(Tc)_4$-TcF_3 in benzonitrile (PhCN) (Figures S75-S77) to examine solvent polarity-dependent photophysical processes. In the case of PhCN, thermal equilibrium between S_1 and CT exists due to the proximity of the energy levels of S_1 and CT states as we already reported in tetracene dimers.[20] This resulted in the smaller Φ_{TrT} in PhCN (Φ_{TrT} = 132 ± 6%) (Table S3) as compared to that in toluene. The rate constants (k_{TrT}) of $^3TcF_3^*+^3TcF_3^*$ deactivation was finally calculated from the lifetime: $\tau_T \approx 0.3$ ms by nsTA, which is quite similar to k_T of $(Tc)_n$ (Table 1, Figures S78-S83). The similar lifetimes of TcF_3-$(Tc)_4$-TcF_3 (τ_{TrT}) and TcF_3-ref (τ_T) also suggested the final exciton trap process (Table 2). These values of τ_{TrT} and τ_T (Table 1) are longer than those of related molecular systems such as tetracene dimers (τ < 5 μs) and perylene oligomers ($\tau \approx 0.1$ ms) reported by Korovina et al.[10b, 21]

To examine the plausible reasons for the improved k_{Diss} and Φ_T, we further performed the temperature-dependent psTA to estimate the thermodynamic parameters for the TT dissociations (Figures S84-S94). The activation enthalpy ($\Delta H^{\ddagger}$) and the

enthalpy change (ΔH) for TT dissociation are represented in the enlarged potential surface (Figure 6A). The detailed discussions for the thermodynamic parameters for the activation state of TT dissociation ($\Delta G^{\ddagger}$, $\Delta H^{\ddagger}$, $\Delta S^{\ddagger}$ and $\Delta\Delta W^{\ddagger}$) are described in SI (Figure S94). The thermodynamic parameters for the activation state of TT dissociation are listed in Table 2.

Then, we also estimated the thermodynamic parameters for TT dissociation (Figure 6B). The thermodynamic parameters for ΔG (ΔH and ΔS) are listed in Table 2. ΔH ≈ +1 kJ mol^{-1} were obtained for Tc-homo-oligomers and TcF_3-$(Tc)_4$-TcF_3 (Table 2). This endothermicity reflects that the TT is stabilized with respect to the T+T due to the charge-transfer (CT) character in the strongly coupled multiexcitons of $^3Tc^*$-$^3Tc^*$ and $^3TcF_3{}^*$-$^3Tc^*$, as reported by our previous studies.[16, 20] Moreover, $\Delta H^{\ddagger} > \Delta H$ (Figure 6A) reveals that conformation changes are essential for the activations. The exergonicity of the TT dissociation ($\Delta G < 0$) in Table 2 is thus originating from the entropy change, i.e., the increased number of the states in the T+T with respect to TT. Accordingly, the ΔS increased as increasing the number of Tc units. Surprisingly, the ΔS of TcF_3-$(Tc)_4$-TcF_3 is much larger than that of $(Tc)_6$ as well as $\Delta S^{\ddagger}$ (Table 2), indicating an important role of the molecular vibration at the trifluorophenyl-substituted tetracene at the terminal positions. Consequently, the ΔG decreased as increasing the number of Tc and the ΔG of TcF_3-$(Tc)_4$-TcF_3 is smaller than that of $(Tc)_6$. The intramolecular dissociation (k_{Diss}) is thus preferential in TcF_3-$(Tc)_4$-TcF_3 due to the increase of ΔS by introduction of trifluorophenyl-substituted energy-acceptors at the terminal positions. This demonstrated the larger entropic gain effect of the trifluorophenyl units relative to the biphenyl linker units.

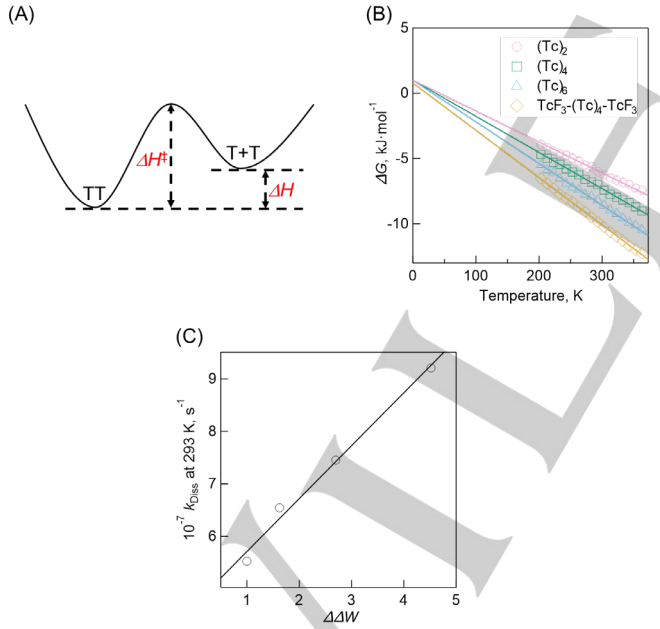

Figure 6. (A) Enlarged potential surface forcusing the TT→T+T dissociation with $\Delta H^{\ddagger}$ and ΔH. (B) The plot of ΔG vs. temperatures. (C) The plot of k_{Diss} vs. $\Delta\Delta W$.

To examine the reason for larger ΔS in $(Tc)_6$ and its enhancement in TcF_3-$(Tc)_4$-TcF_3, we obtained the change of number of T+T with respect to TT by using Boltzmann's equation ($\Delta S = k_B \cdot \ln \Delta W$).[22] For comparison, $\Delta\Delta W$, the relative values of ΔW in other Tc-oligomers to ΔW in $(Tc)_2$, were calculated (Table 2). The increased number of T+T for TT dissociation in TcF_3-$(Tc)_4$-TcF_3 is approximately four times larger than that of $(Tc)_2$. Moreover, we observed a good linear correlation between $\Delta\Delta W$ and k_{Diss} (Figure 6C). Therefore, we successfully demonstrated that the number of activated states increased in $(Tc)_6$ and TcF_3-$(Tc)_4$-TcF_3 due to the increase in the number of Tc and introduction of energy-acceptors at the terminal positions. The enhanced $\Delta\Delta W$ and $\Delta\Delta W^{\ddagger}$ in TcF_3-$(Tc)_4$-TcF_3 are attributable to the increased numbers of separated and activated states in the T+T at -$^3Tc^*$-Tc-$^3TcF_3{}^*$ compared with those in $(Tc)_6$ only by 3,4,5-trifluorophenyl groups replaced with the aliphatic TIPS groups. This is thus attributed to vibrational motions of the aromatic substituent to weaken the CT binding (Figures S56-S57) at TT, as was discussed in the exergonic charge-dissociation processes in organic photovoltaics.[12, 23] This was supported by the vibronic model analysis of TREPR considering the terahertz motions (Figure S67, Table S6).[16, 20] Further discussions about the vibronic coupling of trifluorophenyl unit and other thermodynamic parameters are provided in SI (Figures S93-S94). These thermodynamic parameters strongly support the exciton-migration of ISF and validity of the terminal TcF_3.

Conclusion

In conclusion, this work demonstrates the efficient generation of two individual triplet excitons and exciton-migration process including TT dissociation and exciton-trapping in $(Tc)_n$ and TcF_3-$(Tc)_4$-TcF_3. The Φ_T of $(Tc)_n$ increased up to182 ± 10% with increasing the number of Tc. More importantly, in TcF_3-$(Tc)_4$-TcF_3, the localized triplet excitons at the terminal TcF_3 positions are observed (Φ_{TrT} = 176 ± 8%, τ_{TrT} = 0.30 ms) after the exciton-migration. The thermodynamic parameters were carefully considered. The increased number of possible TT states due to the increased number of Tc moiety and of the vibronic levels by the rotation of the trifluorophenyl group at the terminal TcF_3, leading to the increase in ΔS. Initial singlet exciton-migration would mainly produce the TT states generated by the coupling between $^3Tc^*$ and $^3TcF_3{}^*$ and causes ultimate exciton-trapping by the terminal TcF_3 moieties. Therefore, we successfully demonstrated a molecular design for the efficient exciton-transport process in linear oligomers by promoting TT dissociation and controlling sequential exciton-trapping process. Such thermodynamic control for the exciton-migration associated with SF will provide a new perspective for novel photo-functional systems such as quantum information science and photovoltaics.[4b, 24]

Experimental Section

General and Materials. All solvents and reagents of the best grade available were purchased from commercial suppliers such as Tokyo Chemical Industry, Nacalai Tesque, FUJIFILM Wako Pure Chemical Corporation and Sigma-Aldrich. All commercial reagents were used without further purification. Column flash chromatography was performed on silica gel (Fuji Silysia Chemical LTD., 40-50 μm or 100-210 μm). Preparative recycling gel permeation chromatography was performed with an HPLC apparatus (Japan Analytical Industry LC-9204) by using chloroform as eluent at room temperature. This system is equipped with a pump (JAI PI-60, flow rate 3.0 mL min^{-1}), a UV detector (JAI UV-3740), and two columns (JAIGEL-2H and JAIGEL-1H, both 40 × 600 mm). ^{1}H NMR, ^{13}C NMR and ^{19}F NMR spectra were recorded on a ECS-400 or ALPHA-400 spectrometer using the solvent peak as the reference standard, with chemical shifts given in parts per million. $CDCl_3$ and toluene-d_8 was used as a NMR solvent. MALDI-TOF mass spectra were recorded on Shimadzu MALDI-7090. TcQ-Br, Tc-Br and TcQ were synthesized by using reported method.[25] Br-Tc-Br was synthesized by using reported method.[14a] Tc-ref was synthesized by using reported method.[26] $(Tc)_2$ was synthesized by using reported method.[11]

Spectroscopic Measurements. UV-VIS absorption spectra were recorded on Agilent (8453) UV-VIS-NIR spectrophotometer. Fluorescence spectra were recorded on JASCO (FP-8600) spectrofluorophotometer.

Femtosecond Pump-Probe System. The transient absorption spectroscopy measurements were carried out using a femtosecond pump–probe system. A Libra F laser system (Coherent Inc.) was used to create fundamental light pulses at 800 nm at a repetition rate of 1 kHz. The pulse energy was 1 mJ, and the pulse duration was approximately 100 fs. The fundamental beam was split in two, and the majority of the beam energy (roughly 90%) was directed to a Topas C optical parametric amplifier (Light Conversion Ltd.) to produce excitation pulses at the desired wavelength. The rest of the fundamental beam was delivered to a white continuum generator (sapphire crystal) for sample probing. The probe beam was split in two to record reference and signal responses. The measurement system (ExciPro, CDP Inc.) was equipped with a silicon CCD array for measurements in the visible part of the spectrum. The measurements were carried out by comparing responses with and without excitation using a chopper synchronized with the fundamental laser pulses. The spectra were typically acquired by recording 5000 shots, i.e. averaging over 5 s. Excitation energies were sufficiently low to avoid multiple exciton generation; this was verified by recording a series of measurements with different excitation energies for the same sample. No excitation energy dependence of the response was observed.

Picosecond Transient Absorption Measurement. Picosecond transient absorption measurements were conducted using the device manufactured by Unisoku Co., Ltd. Measurement method used in this instrument was Randomly Interleaved Pulse Train Method.[27] Temperature-dependent psTA measurements were measured by using CoolSpek USP-203-SH-ST (Unisoku Co., Ltd).

Time Resolved Electron Paramagnetic Resonance Measurement. The X–band TREPR measurements were performed using a Bruker EMX Plus system in which a modified wide-band preamplifier was equipped in the microwave bridge. The field modulation was not employed. The second harmonics (532 nm) of a Nd:YAG laser (Continuum Minilite II, fwhm = 5 ns) were used to light excitation. A laser de-polarizer (SIGMA KOKI, DEQ 1N) was placed between the laser exit and the microwave cavity for the depolarized TREPR data. Transient EPR signals were averaged by a Tektronix DPO3054 500 MHz digital phosphor oscilloscope at 201 different external magnetic field positions. Temperature was controlled by a cryostat system (Oxford, ESR900) by using liquid nitrogen as the cryogen.

Acknowledgements

This work was partially supported by JSPS KAKENHI Grant-in-Aid for Transformative Research Areas, “Dynamic Exciton” (JP20H05832 to Y.K. and JP21H05403 to T.H.) and Grant Nos. JP19H00888, JP20K21174 to Y.K, JP18H01957, JP18K19063, JP20H05234, JP20KK0120, JP21H01908, JP21K19011, 22H04558 to T.H., JP20K05652 to H.S. and JP20J13133 to S.N. This work was partially carried out by the joint research program of Molecular Photoscience Research Center, Kobe University and the Research Program of "Five-star Alliance" in "NJRC Mater. & Dev."

Keywords: Singlet Fission • Tetracene • Oligomer • Exciton-Transport • Vibronic Coupling

[1] a) T. Mirkovic, E. E. Ostroumov, J. M. Anna, R. Van Grondelle, Govindjee, G. D. Scholes, *Chem. Rev.* **2017**, *117*, 249-293; b) N. Aratani, D. Kim, A. Osuka, *Acc. Chem. Res.* **2009**, *42*, 1922-1934; c) C.-K. Yong, P. Parkinson, D. V. Kondratuk, W.-H. Chen, A. Stannard, A. Summerfield, J. K. Sprafke, M. C. O'Sullivan, P. H. Beton, H. L. Anderson, L. M. Herz, *Chem. Sci.* **2015**, *6*, 181-189.

[2] a) V. Coropceanu, J. Cornil, D. A. Da Silva Filho, Y. Olivier, R. Silbey, J.-L. Brédas, *Chem. Rev.* **2007**, *107*, 926-952; b) J.-L. Brédas, J. E. Norton, J. Cornil, V. Coropceanu, *Acc. Chem. Res.* **2009**, *42*, 1691-1699; c) A. Saeki, Y. Koizumi, T. Aida, S. Seki, *Acc. Chem. Res.* **2012**, *45*, 1193-1202.

[3] a) O. V. Mikhnenko, P. W. M. Blom, T.-Q. Nguyen, *Energy Environ. Sci.* **2015**, *8*, 1867-1888; b) R. Nagata, H. Nakanotani, W. J. Potscavage, C. Adachi, *Adv. Mater.* **2018**, *30*, 1801484.

[4] a) B. K. Rugg, M. D. Krzyaniak, B. T. Phelan, M. A. Ratner, R. M. Young, M. R. Wasielewski, *Nat. Chem.* **2019**, *11*, 981-986; b) S. Matsuda, S. Oyama, Y. Kobori, *Chem. Sci.* **2020**, *11*, 2934-2942.

[5] a) Q. Zhou, T. M. Swager, *J. Am. Chem. Soc.* **1995**, *117*, 12593-12602; b) N. Aratani, H. S. Cho, T. K. Ahn, S. Cho, D. Kim, H. Sumi, A. Osuka, *J. Am. Chem. Soc.* **2003**, *125*, 9668-9681; c) A. Ajayaghosh, V. K. Praveen, C. Vijayakumar, S. J. George, *Angew. Chem. Int. Ed.* **2007**, *46*, 6260-6265.

[6] C. D. Dimitrakopoulos, P. R. L. Malenfant, *Adv. Mater.* **2002**, *14*, 99-117.

[7] a) M. B. Smith, J. Michl, *Chem. Rev.* **2010**, *110*, 6891-6936; b) K. Miyata, F. S. Conrad-Burton, F. L. Geyer, X. Y. Zhu, *Chem. Rev.* **2019**, *119*, 4261-4292.

[8] a) N. R. Monahan, D. Sun, H. Tamura, K. W. Williams, B. Xu, Y. Zhong, B. Kumar, C. Nuckolls, A. R. Harutyunyan, G. Chen, H.-L. Dai, D. Beljonne, Y. Rao, X. Y. Zhu, *Nat. Chem.* **2017**, *9*, 341-346; b) N. Alagna, J. Han, N. Wollscheid, J. L. Perez Lustres, J. Herz, S. Hahn, S. Koser, F. Paulus, U. H. F. Bunz, A. Dreuw, T. Buckup, M. Motzkus, *J. Am. Chem. Soc.* **2019**, *141*, 8834-8845; c) C. Hetzer, B. S. Basel, S. M. Kopp, F. Hampel, F. J. White, T. Clark, D. M. Guldi, R. R. Tykwinski, *Angew. Chem. Int. Ed.* **2019**, *58*, 15263-15267; d) A. T. Gilligan, E. G. Miller, T. Sammakia, N. H. Damrauer, *J. Am. Chem. Soc.* **2019**, *141*, 5961-5971; e) J. Kim, H. T. Teo, Y. Hong, J. Oh, H. Kim, C. Chi, D. Kim, *Angew. Chem. Int. Ed.* **2020**, *59*, 20956-20964; f) S. Paul, C. Govind, V. Karunakaran, *J. Phys. Chem. B* **2021**, *125*, 231-239; g) M. Dvořák, S. K. K. Prasad, C. B. Dover, C. R. Forest, A. Kaleem, R. W. MacQueen, A. J. Petty, R. Forecast, J. E. Beves, J. E. Anthony, M. J. Y. Tayebjee, A. Widmer-Cooper, P. Thordarson, T. W. Schmidt, *J. Am. Chem. Soc.* **2021**, *143*, 13749-13758.

[9] H. L. Stern, A. J. Musser, S. Gelinas, P. Parkinson, L. M. Herz, M. J. Bruzek, J. Anthony, R. H. Friend, B. J. Walker, *Proc. Natl. Acad. Sci. U. S. A.* **2015**, *112*, 7656-7661.

[10] a) L. M. Yablon, S. N. Sanders, H. Li, K. R. Parenti, E. Kumarasamy, K. J. Fallon, M. J. A. Hore, A. Cacciuto, M. Y. Sfeir, L. M. Campos, *J. Am. Chem. Soc.* **2019**, *141*, 9564-9569; b) N. V. Korovina, C. H. Chang, J. C. Johnson, *Nat. Chem.* **2020**, *12*, 391-398; c) Z. Wang, H. Liu, X. Xie, C. Zhang, R. Wang, L. Chen, Y. Xu, H. Ma, W. Fang, Y. Yao, H. Sang, X. Wang, X. Li, M. Xiao, *Nat. Chem.* **2021**, *13*, 559-567; d) G. He, L. M. Yablon, K. R. Parenti, K. J. Fallon, L. M. Campos, M. Y. Sfeir, *J. Am. Chem. Soc.* **2022**, *144*, 3269-3278; e) M. Fumanal, C. Corminboeuf, *Chem. Mater.* **2022**, *34*, 4115-4121.

[11] S. Nakamura, H. Sakai, H. Nagashima, Y. Kobori, N. V. Tkachenko, T. Hasobe, *ACS Energy Lett.* **2019**, *4*, 26-31.

[12] T. Miura, R. Tao, S. Shibata, T. Umeyama, T. Tachikawa, H. Imahori, Y. Kobori, *J. Am. Chem. Soc.* **2016**, *138*, 5879-5885.

[13] S. Nakamura, H. Sakai, M. Fuki, Y. Kobori, N. V. Tkachenko, T. Hasobe, *J. Phys. Chem. Lett.* **2021**, *12*, 6457-6463.

[14] a) A. B. Pun, S. N. Sanders, E. Kumarasamy, M. Y. Sfeir, D. N. Congreve, L. M. Campos, *Adv. Mater.* **2017**, *29*, 1701416; b) A. B. Pun, A. Asadpoordarvish, E. Kumarasamy, M. J. Y. Tayebjee, D. Niesner, D. R. McCamey, S. N. Sanders, L. M. Campos, M. Y. Sfeir, *Nat. Chem.* **2019**, *11*, 821-828.

[15] a) A. M. Müller, Y. S. Avlasevich, W. W. Schoeller, K. Müllen, C. J. Bardeen, *J. Am. Chem. Soc.* **2007**, *129*, 14240-14250; b) Y. Matsui, S. Kawaoka, H. Nagashima, T. Nakagawa, N. Okamura, T. Ogaki, E. Ohta, S. Akimoto, A. Sato-Tomita, S. Yagi, Y. Kobori, H. Ikeda, *J. Phys. Chem. C* **2019**, *123*, 18813-18823; c) A. B. Pun, S. N. Sanders, M. Y. Sfeir, L. M. Campos, D. N. Congreve, *Chem. Sci.* **2019**, *10*, 3969-3975.

[16] Y. Kobori, M. Fuki, S. Nakamura, T. Hasobe, *J. Phys. Chem. B* **2020**, *124*, 9411-9419.

[17] a) D. G. Bossanyi, Y. Sasaki, S. Wang, D. Chekulaev, N. Kimizuka, N. Yanai, J. Clark, *JACS Au* **2021**, *1*, 2188-2201; b) R. M. Jacobberger, Y. Qiu, M. L. Williams, M. D. Krzyaniak, M. R. Wasielewski, *J. Am. Chem. Soc.* **2022**, *144*, 2276-2283.

[18] a) I. H. M. van Stokkum, D. S. Larsen, R. van Grondelle, *Biochim. Biophys. Acta, Bioenerg.* **2004**, *1657*, 82-104; b) J. J. Snellenburg, S. Laptenok, R. Seger, K. M. Mullen, I. H. M. van Stokkum, *J. Stat. Softw.* **2012**, *49*, 1-22.

[19] a) W.-L. Chan, M. Ligges, A. Jailaubekov, L. Kaake, L. Miaja-Avila, X.-Y. Zhu, *Science* **2011**, *334*, 1541-1545; b) H. L. Stern, A. Cheminal, S. R. Yost, K. Broch, S. L. Bayliss, K. Chen, M. Tabachnyk, K. Thorley, N. Greenham, J. M. Hodgkiss, J. Anthony, M. Head-Gordon, A. J. Musser, A. Rao, R. H. Friend, *Nat. Chem.* **2017**, *9*, 1205-1212.

[20] S. Nakamura, H. Sakai, H. Nagashima, M. Fuki, K. Onishi, R. Khan, Y. Kobori, N. V. Tkachenko, T. Hasobe, *J. Phys. Chem. C* **2021**, *125*, 18287-18296.

[21] a) N. V. Korovina, J. Joy, X. Feng, C. Feltenberger, A. I. Krylov, S. E. Bradforth, M. E. Thompson, *J. Am. Chem. Soc.* **2018**, *140*, 10179-10190; b) N. V. Korovina, N. F. Pompetti, J. C. Johnson, *J. Chem. Phys.* **2020**, *152*, 040904.
[22] W.-L. Chan, M. Ligges, X. Y. Zhu, *Nat. Chem.* **2012**, *4*, 840-845.
[23] H. Imahori, Y. Kobori, H. Kaji, *Acc. Mater. Res.* **2021**, *2*, 501-514.
[24] K. E. Smyser, J. D. Eaves, *Sci. Rep.* **2020**, *10*, 18480.
[25] S. N. Sanders, E. Kumarasamy, A. B. Pun, M. L. Steigerwald, M. Y. Sfeir, L. M. Campos, *Angew. Chem. Int. Ed.* **2016**, *55*, 3373-3377.
[26] W. Fudickar, T. Linker, *J. Am. Chem. Soc.* **2012**, *134*, 15071-15082.
[27] T. Nakagawa, K. Okamoto, H. Hanada, R. Katoh, *Opt. Lett.* **2016**, *41*, 1498-1501.

Entry for the Table of Contents

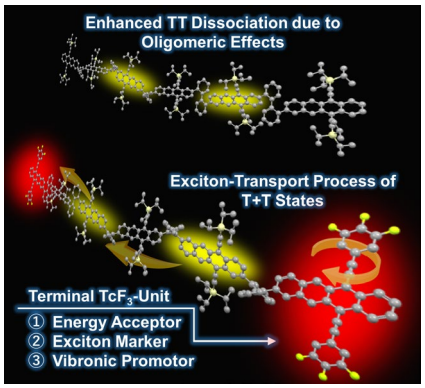

We newly synthesized a series of homo- and hetero-tetracene (Tc) oligomers to propose a molecular design strategy for the ~~highly~~ efficient exciton-transport process in linear oligomers by promoting correlated triplet pair (TT) dissociation and controlling sequential exciton-trapping process of individual doubled triplet excitons (T+T) by intramolecular singlet fission.